Entropy, local order, and the freezing transition in Morse liquids

Somendra Nath Chakraborty and Charusita Chakravarty*
Department of Chemistry, Indian Institute of Technology Delhi, New Delhi 110016, India
(Received 9 April 2007; published 13 July 2007)

The behavior of the excess entropy of Morse and Lennard-Jones liquids is examined as a function of temperature, density, and the structural order metrics. The dominant pair correlation contribution to the excess entropy is estimated from simulation data for the radial distribution function. The pair correlation entropy (S_2) of these simple liquids is shown to have a threshold value of $(-3.5\pm0.3)k_B$ at freezing. Moreover, S_2 shows a $T^{-2/5}$ temperature dependence. The temperature dependence of the pair correlation entropy as well as the behavior at freezing closely correspond to earlier predictions, based on density functional theory, for the excess entropy of repulsive inverse power and Yukawa potentials [Rosenfeld, Phys. Rev. E **62**, 7524 (2000)]. The correlation between the pair correlation entropy and the local translational and bond orientational order parameters is examined, and, in the case of the bond orientational order, is shown to be sensitive to the definition of the nearest neighbors. The order map between translational and bond orientational order for Morse liquids and solids shows a very similar pattern to that seen in Lennard-Jones-type systems.

DOI: 10.1103/PhysRevE.76.011201 PACS number(s): 61.20.Qg, 64.70.Pf, 66.10.Cb

I. INTRODUCTION

The structure of simple liquids is dominated by strong, short-range repulsive interactions, rather than by weak, long-range attractive interactions. If the interparticle interactions in such a system are isotropic, as in the cases of rare gases and spherical colloids, the structure can be described in terms of random, close-packing arrangements of spheres [1,2]. Monatomic liquids show a fairly wide range of variation in the strength of the melting transition, as indexed by the change in molar entropies, ΔS_{fus}, and volume, ΔV_{fus}, on fusion [3,4]. Experimental data on melting of atomic systems suggests that systems with soft, long-range metallic interactions, such as alkali metals, typically show a weak melting transition, with a 2–3% change in density on melting, while van der Waals bonded systems, such as rare gases, show a much stronger melting transition, with a 16% change in density [5,6]. Variable-range Morse systems provide a convenient set of systems to model this variation in melting behavior in atomic systems as a function of correlated changes in range and curvature of the interparticle potentials [7]. The Morse pair interaction is characterized by a size parameter r_e, the well depth of the pair potential, ϵ, and a range parameter α, which controls both the range of the pair potential as well as its curvature or softness [8–12]. The variation in melting behavior is accompanied by characteristic changes in the potential energy landscape of Morse liquids, as indexed by statistical properties of inherent structures, stationary points, and the instantaneous normal mode spectrum [13–16]. In this paper, we examine the relationship between entropy and degree of disorder in Morse liquids, with a view to understanding some of the quantitative connections between excess entropy, diffusivity, and local order in liquids that have emerged in the past decade.

In the case of classical liquids, the crucial thermodynamic quantity is the excess entropy S_e, defined as the entropy difference between the liquid and the ideal gas states. The quantity $\exp(S_e)$ can be treated as a measure of the number of accessible configurations. It is possible to decompose S_e into separate contributions from n-body correlation functions [17–22]:

$$S_e = S_2 + S_3 + \cdots + S_n + \cdots, \tag{1}$$

where S_2 is the pair correlation entropy, and $\Delta S_R = S_e - S_2$ is defined as the residual multiparticle entropy. The pair correlation entropy forms the dominant contribution, of the order of 85–90%, in the case of simple, one-component liquids, and can be written as

$$S_2 = -2\pi\rho \int_0^\infty \{g(r)\ln g(r) - [g(r)-1]\} r^2 dr, \tag{2}$$

where $g(r)$ is the pair correlation function, r is the pair separation distance, and S_2 is given in units of k_B per particle. Since $g(r)$ is a readily measurable quantity in either experiments or simulations, S_2 provides a convenient and reasonably accurate structural measure of the thermodynamic excess entropy. This is particularly important in the case of liquids, since many transport properties, such as the diffusivity, viscosity, and thermal conductivity, obey excess-entropy-based scaling relationships [23–27]. In the case of a monatomic liquid at temperature T and density ρ, the diffusivity (D) scales as

$$D^* = D\frac{\rho^{1/3}}{(k_B T/m)^{1/2}} = A\exp(\alpha S_e), \tag{3}$$

where we have used a macroscopic scaling parameter for the diffusivity. Most simple liquids obey the more precise Dzugutov scaling law, which uses microscopic reduction parameters, and is stated as

$$D_\Gamma^* = D/(\sigma^2\Gamma_E) = 0.049\exp(S_e), \tag{4}$$

where σ is the location of the first maximum of pair correlation function $g(r)$ and Γ_E is the collision frequency accord-

*charus@chemistry.iitd.ernet.in

ing to Enskog theory [28]. Such scaling relationships have been found to hold also for confined fluids and anomalous liquids, such as molten silica [29–32]. Recently, an effort has been made to understand the relationship between diffusivity and excess entropy in terms of properties of the underlying potential energy landscape [33].

The variations in the excess entropy as a function of the macroscopic variables must be related to the behavior of different order metrics characterizing the nature as well as the extent of structural disorder in liquids and glasses. A measure of configurational ordering in liquids is provided by the deviation of the pair correlation function from the uniform value of unity seen in an ideal gas [34–38]. This is quantified using a translational or density-induced order parameter defined as

$$\tau = \frac{1}{s_c}\int_0^{s_c} |g(s) - 1| ds, \tag{5}$$

where $s = r\rho^{1/3}$ is the radial distance scaled by the number density (ρ), $g(s)$ is the pair correlation function, and s_c is a cutoff distance. By definition, S_2 and τ are expected to be anticorrelated. Bond orientational order parameters, originally formulated to quantify global structural anisotropy in liquid crystals and solids [39], are convenient for measuring the local anisotropy in the neighborhood of a given atom. The orientation of a bond vector $\mathbf{r}$ joining an atom with neighbor lying within a cutoff distance R_c, relative to a space-fixed reference frame, is denoted by the spherical polar angles $\theta(\mathbf{r})$ and $\phi(\mathbf{r})$. With each bond surrounding a given atom, one can associate a spherical harmonic $Y_{lm}[\theta(\mathbf{r}), \phi(\mathbf{r})]$. By summing over all the bonds connecting a given atom with its neighbors, one can define a local quantity

$$q_{lm}(\mathbf{r}) = (1/n_b)\sum_i Y_{lm}[\theta(\mathbf{r}_i), \phi(\mathbf{r}_i)], \tag{6}$$

where n_b denotes the number of nearest neighbors of the atom. To construct a rotationally invariant local order parameter [40], one then defines q_l as

$$q_l = \left(\frac{4\pi}{(2l+1)}\sum_{m=-l}^{l} |q_{lm}|^2\right)^{1/2}. \tag{7}$$

The q_6 order parameter is large when particles are in icosahedral, face-centered cubic, or hexagonally close-packed environment [39,40]. In the case of disordered systems where interparticle interactions impose a strong local symmetry preference, as in the case of tetrahedral, network-forming liquids and glasses, it is convenient to introduce other measures of orientational order [41,42]. In the case of liquids with waterlike anomalies, it can be shown that variations in excess entropy reflect the interplay of competing local orientational ordering preferences and result in a related set of structural, diffusional, and density anomalies [31,43–47].

For simple liquids, it is possible to define freezing criteria based on the pair correlation as well as multiparticle correlation contributions to the configurational excess entropy. The residual multiparticle excess entropy (RMPE) criterion states that $S_R = S_e - S_2$ vanishes when a disordered or partially ordered fluid phase transforms into an ordered phase [48–51]. Even though S_R makes only a small quantitative contribution to the total excess entropy, the RMPE criterion is found to be a reasonable predictor of the freezing transition of a number of liquids, including Gaussian-core models which show a pressure-driven reentrant transition. Less attention has been focused on the behavior of the pair correlation entropy S_2 near freezing, even though the work of Rosenfeld and co-workers shows that the excess entropy at freezing of all inverse power and Yukawa fluids at freezing is $-4k_B$. Other than a demonstration by Yokohama that $S_e \approx S_2 \approx -3.5k_B$ for some liquid metals [52], we are not aware of any tests of this freezing rule in the literature. There is clearly an interesting connection between this excess-entropy-based freezing criterion and the well-known Hansen-Verlet freezing rule, which correlates the freezing transition with the first maximum of the static structure factor reaching a threshold value of 2.89.

In this paper, we examine the behavior of the pair correlation entropy as a function of the temperature, density, and local order metrics for a set of Morse liquids. Since the pair correlation entropy is a good estimator of the excess entropy, we can use our results for Morse liquids to test excess-entropy-based freezing criteria and temperature scalings predicted by Rosenfeld and co-workers using density functional calculations for repulsive soft-sphere and Yukawa liquids [27]. The relationship between excess entropy and orientational order, which has been largely examined in the context of liquids with waterlike anomalies, is discussed for this range of simple liquids. We also determine the order map for these variable-range Morse liquids, and compare it with that of Lennard-Jones and hard-sphere systems derived previously [38].

II. COMPUTATIONAL DETAILS

The potential energy surface is assumed to be pair additive, i.e.,

$$U(\mathbf{r}) = \frac{1}{2}\sum_{i=1}^{N}\sum_{j\neq i} u_2(r_{ij}), \tag{8}$$

where $\mathbf{r}$ denotes the $3N$ position coordinates of the N-particle system, and u_2 is a pair potential that depends only on the distance r_{ij} between atoms i and j. In this work, we take u_2 to be either the Morse, Lennard-Jones (u_{LJ}), or smoothed Lennard-Jones (SLJ) pair potential.

The Morse potential is defined as

$$u_M(r) = \epsilon\left\{\exp\left[-\alpha\left(\frac{r}{r_e} - 1\right)\right] - 1\right\}^2 - \epsilon, \tag{9}$$

where ϵ is the well depth, r_e is the equilibrium pair separation, and α is a dimensionless range parameter [8]. The higher the value of α, the shorter the range of the potential and the steeper the curvature $\sqrt{2\epsilon\alpha^2/r_e^2}$ at $r = r_e$. The reduced units of length and energy for the Morse systems are taken as r_e and ϵ, respectively. Morse parameters can be tuned to fit bulk and diatomic data for a wide range of systems [10,11]. Metals such as sodium and nickel have range parameters of

TABLE I. Solid-liquid coexistence properties along the melting line for the Lennard-Jones (LJ), smoothed Lennard-Jones (SLJ), and Morse (M_α) systems [7,54,58]. All quantities are expressed in reduced units of r_e and ϵ.

System	T_m	P_m	ρ_l	ρ_s	S_2	ΔH_m	ΔS_m	$\Delta\rho_m/\rho_s$	R_c	Q_c
$\alpha=4$	0.636	0.947	1.70	1.78	−3.29	0.582	0.91	0.045	3.30	1.14
$\alpha=5$	0.657	0.947	1.33	1.44	−3.36	0.759	1.15	0.076	3.61	1.27
$\alpha=6$	0.679	0.947	1.19	1.33	−3.31	0.979	1.44	0.105	3.70	1.29
$\alpha=7$	0.687	0.947	1.11	1.30	−3.35	1.249	1.81	0.146	3.80	1.32
$\alpha=9$	0.696	0.947	1.01	1.28	−3.24	2.490	3.58	0.210	3.85	1.35
LJ	0.780	0.947	1.21	1.36	−3.38	1.142	1.46	0.110	2.25	1.26
SLJ	0.670	0.947	1.18	1.34	−3.31	1.054	1.57	0.116	2.25	1.36
	0.704	1.544	1.20	1.34	−3.34	1.057	1.50	0.109	2.25	1.36
	0.793	3.169	1.24	1.37	−3.43	1.123	1.41	0.097	2.25	1.36

3.15 and 3.95, respectively, while the very short-ranged C_{60} potential has a range parameter of 13.62. van der Waals bonded systems such as the rare gases have range parameters close to 6. This is consistent with the fact that, provided the well depths and equilibrium pair separations of the Morse and Lennard-Jones pair interactions are chosen to coincide, the curvature at r_e for both functions will be the same for $\alpha=6$. Morse systems with α values of 4, 5, 6, 7, and 9 are studied in this work. We refer to a Morse system with a parameter α as an M_α system.

We compare our results for the Morse systems with those for the LJ system, which has been extensively studied in the literature [53,54]. The LJ pair potential is written in its standard form as

$$u_{LJ}(r) = 4\epsilon\left[\left(\frac{\sigma}{r}\right)^{12} - \left(\frac{\sigma}{r}\right)^{6}\right], \tag{10}$$

where ϵ is the well depth and σ is the value of r for which $u_{LJ}(r)=0$. To facilitate comparison with the results for Morse liquids, in this work, we take the reduced units of length and energy for the LJ system as $r_e=2^{1/6}\sigma$ and ϵ, respectively.

The smoothed 12-6 Lennard-Jones pair potential $u_{SLJ}(r)$ is defined as [55]

$$u(r) = \begin{cases} A\left\{\left(\frac{1}{r}\right)^{12} - \left(\frac{1}{r}\right)^{5}\right\} \exp[1/(r-a)] & \text{for } 0 < r \leqslant a, \quad (11) \\ 0 & \text{for } r > a, \quad (12) \end{cases}$$

where r is the interparticle separation. The parameter a fixes the length of the interaction, so that the attraction is smoothly truncated to zero at $r=a$. The parameters A and a are chosen to reproduce the location and depth of the minimum in the 12-6 Lennard-Jones potential, and are set to $A=6.767\,441$ and $a=2.464\,918\,32$. The derivatives of the potential to all orders are continuous at the cutoff, which makes it particularly suitable for local minimizations. The reduced units of length and energy are taken to be the equilibrium pair separation and the well depth, as in the case of the LJ and Morse systems.

For all three classes of interaction potentials (M_α, LJ, and SLJ), we use isothermal-isobaric (*NPT*) ensemble simulations at a common reduced pressure of $0.947r_e^3/\epsilon$. To implement the *NPT* algorithm [56,57], trial Monte Carlo (MC) configurations are generated using two types of moves: (i) *volume moves*, in which a change in the simulation cell volume is made by sampling with respect to $\ln v$, keeping particle positions and Fourier coefficients constant, and (ii) *particle moves*, in which the coordinates of a single particle are moved, keeping all other variables constant. The percentage of volume moves was kept between 10% and 15%. Equilibration and production run lengths both typically contained 5×10^6 trial configurations.

For the Morse and Lennard-Jones liquids, a simulation cell with 343 particles with rhombic dodecahedral periodic boundary conditions was used [56]. In the case of the smoothed Lennard-Jones liquid, a 256-particle simulation cell with cubic periodic boundary conditions was used. A spherical potential cutoff R_c and standard long-range corrections were employed for the LJ and M_α systems. In the case of the SLJ system, the pair interaction is defined to be zero for $R_c \geqslant a$ and no long-range corrections are necessary. The potential cutoff distance R_c was initialized at the start of the run, but when volume moves were made, it was scaled appropriately. Table I reports the mean values of R_c in our simulations. Additional details regarding the Monte Carlo simulations can be found in our previous papers [7,58]. Fig-

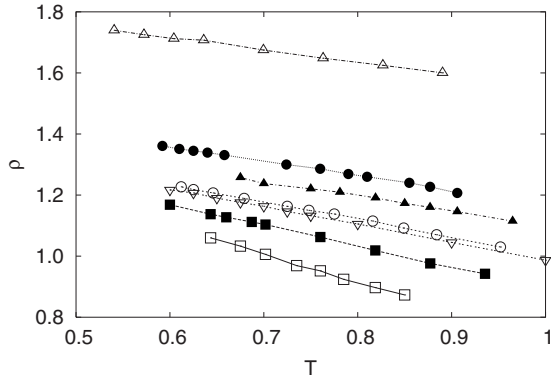

FIG. 1. Temperature (T) dependence of number density (ρ) for Morse (M_α), Lennard-Jones (LJ), and smoothed Lennard-Jones (SLJ) liquids along the $P=0.947$ isobar. The systems are denoted using the following symbols: M_9 (□), M_7 (■), M_6 (○), M_5 (●), M_4 (△), LJ (▲), SLJ (▽).

ure 1 shows the variation in density with temperature along the $P=0.947$ isobar for all the systems studied in this work. A limited number of Monte Carlo simulations have also been performed for soft-sphere (SS) systems with $u_2(r)=\epsilon(\sigma/r)^n$, using a cubic simulation cell with 256 particles and a long-range potential cutoff [59].

To facilitate comparisons with our previous work on excess entropy in liquids [33,58,60], we have used results from microcanonical (*NVE*) ensemble molecular dynamics (MD) simulations of LJ and SLJ liquids. The MD simulations were performed for 256 particles using cubic periodic boundary conditions. The time step was kept at 0.003 reduced units, and the equilibration and productions runs used 5000 and 3000 time steps, respectively. Canonical ensemble (*NVT*) molecular dynamics simulations of the Lennard-Jones liquid are also reported here for isotherms at $T=0.75$, 1.00, and 1.25.

1000 configurations were sampled from each of the runs, and calculations for excess entropy, translational, and bond orientational order were done. The translational order was evaluated using Eq. (1); for all the systems, the bin size for integration was kept at $0.001r_e$, and the upper limit for the integration over the pair distance r was set to $3.5\rho^{-1/3}$. When computing the excess entropy using Eq. (2), the bin size was kept at $0.001r_e$, and the upper limit for integration was kept at $3.5r_e$ for all the Morse, LJ, and SLJ liquids, except the M_4 system, for which it was set at $3.1r_e$. Bond orientational order is sensitive to the criteria used to define nearest neighbors. Following the work of Steinhardt *et al.*, we initially defined nearest neighbors of a given atoms as all atoms lying within a cutoff distance Q_c, determined by the location of the first minimum of the pair correlation function. In the *NPT* simulations, Q_c, like R_c, was scaled after a volume move; the mean value of Q_c for each system along the $P=0.947$ isobar is given in Tables I and II. In most of the results presented here, we have used this definition. However, more recently, it has been suggested that for liquids with local, distorted icosahedral order it might be useful to consider the summation in Eq. (6) to be over the 12 nearest neighbors [43–45]. We have compared the results using both the definitions.

In order to study the behavior of the liquids in the vicinity of the freezing transition, we have used information on solid-liquid coexistence conditions determined in previous studies. The melting temperatures of the Morse solids along the $P=0.947$ isobar were computed using a Landau free energy curve approach [7]. In the case of the Lennard-Jones and soft-sphere systems, the melting lines as determined by Agrawal and Kofke were used [54,59]. Three points along the melting line of the SLJ system were determined using thermodynamic perturbation theory [58]. The thermodynamic properties of the melting transition at the state points studied in this work are shown in Tables I and II.

With regard to the results presented in the next section, all figures comparing Morse and Lennard-Jones systems are from *NPT*-ensemble simulations and correspond to a common reduced pressure of $0.947r_e^3/\epsilon$. For the Lennard-Jones system, some of the figures compare the results for isotherms corresponding to isobaric and isochoric variations in temperature.

III. RESULTS AND DISCUSSION

Figure 2(a) shows the dependence of the pair correlation entropy S_2 of Morse and Lennard-Jones liquids on number density along the $P=0.947$ isobar. S_2 decreases monotonically with ρ along each isobar, as expected in the case of simple liquids. The curves for the $\alpha=6$ Morse (M_6) liquid and the Lennard-Jones and the smooth Lennard-Jones systems lie very close together, indicating that the dominant effect that determines the $S_2(\rho)$ curves is the curvature of the pair interaction near the minimum and consequently the structure in the $g(r)$ associated with the nearest-neighbor shells. For a fixed value of the pair correlation entropy, the

TABLE II. Solid-fluid coexistence data for soft-sphere or inverse power $[\epsilon(\sigma/r)^n]$ potentials [59]. Quantities are expressed in reduced units.

$1/n$	P	ρ_l	ρ_s	S_2	ΔH_m	ΔS_m	$\Delta\rho_m/\rho_s$	R_c	Q_c
0.05	21.66	1.406	1.49	−3.87	1.03	1.0382	0.059	2.75	1.39
0.06	45.97	1.458	1.54	−3.76	0.93	0.9491	0.052	2.72	1.39
0.07	19.58	1.527	1.60	−3.66	0.94	0.9313	0.050	2.70	1.39
0.08	27.69	1.616	1.62	−3.75	0.84	0.8316	0.046	2.65	1.39
0.09	36.98	1.778	1.72	−3.71	0.86	0.7331	0.034	2.60	1.39
0.10	43.32	1.892	1.84	−3.72	0.88	0.6603	0.027	2.50	1.39

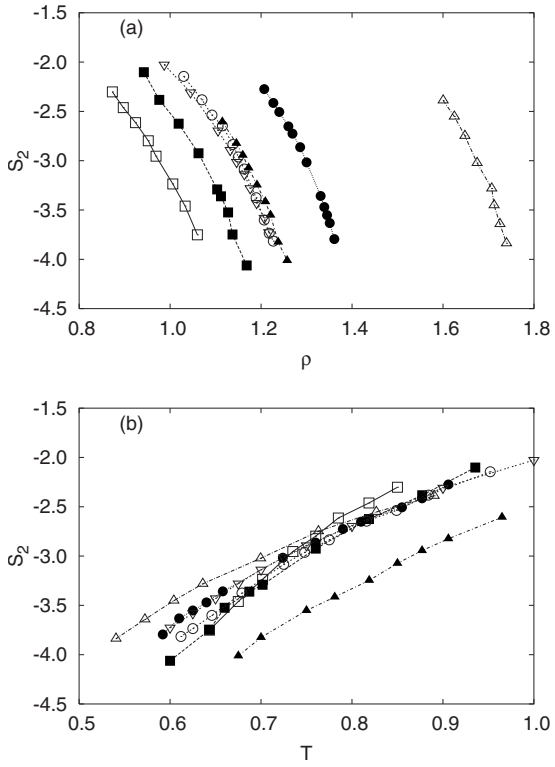

FIG. 2. Dependence of pair correlation entropy (S_2) on (a) number density (ρ) and (b) temperature (T) for Morse (M_α), Lennard-Jones (LJ), and smoothed Lennard-Jones (SLJ) liquids along the $P=0.947$ isobar. The systems are denoted using the following symbols: M_9 (□), M_7 (■), M_6 (○), M_5 (●), M_4 (△), LJ (▲), SLJ (▽).

soft, relatively long-range M_4 system has the maximum value of density, while the short-range M_9 system has the lowest density. Systems with large curvature in the neighborhood of the minimum have more structured pair correlation functions and lower excess entropies at a given density.

Figure 2(b) shows the dependence of S_2 on the temperature T. In contrast to the case of the density dependence, the $S_2(T)$ curves are not ordered according to the curvature in the neighborhood of the minimum. The Lennard-Jones system, which has a long-range r^{-6} tail, has a lower entropy at any given temperature than any of the other systems. It is interesting that the SLJ system, which has a finite cutoff, has an $S_2(T)$ curve that is intermediate between that of the M_5 and M_6 liquids, which have an exponentially decaying long-range tail. A comparison of Figs. 2(a) and 2(b) indicates that the ρ and T dependence highlight different aspects of the interaction potential, e.g., the curvature distribution near the equilibrium pair separation as opposed to the behavior of the long-range tail.

We have computed the pair correlation entropy S_2 of Lennard-Jones, smoothed Lennard-Jones, Morse, and inverse power liquids at known solid-liquid thermodynamic coexistence points. The results for all the systems studied here are summarized in Tables I and II as well as Fig. 3, and it is evident that S_2/k_B at freezing is approximately $-3.5(\pm 0.3)k_B$ for all the systems. S_e at freezing for the soft-sphere systems was determined to be approximately $-4k_B$ by Rosenfeld and the S_2 value is only marginally higher at $-3.8k_B$. The results

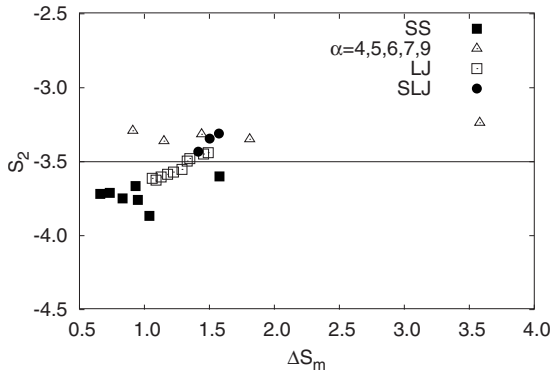

FIG. 3. Pair correlation entropy (S_2) of liquid at freezing versus the thermodynamic entropy of melting (ΔS_m). Solid-liquid coexistence conditions for M_α, LJ, and SLJ systems are taken from Refs. [7,54,58], respectively. Also shown are the solid-fluid coexistence results for the soft-sphere (SS) system for n lying between 8 and 20 [59].

in Fig. 3 suggest that the pair correlation entropy reaches has a value of $-3.5k_B$, within an error bar of approximately 10%, for a wide range of systems.

Earlier studies on inverse power and repulsive Yukawa potentials suggest that the excess entropy must show a $T^{-(2/5)}$ scaling. We test this relationship for the Morse, LJ, and SLJ systems along the $P=0.947$ isobar in Fig. 4(a) by fitting S_2 to the functional form $mT^{-0.4}+c$. As shown in Table III, the

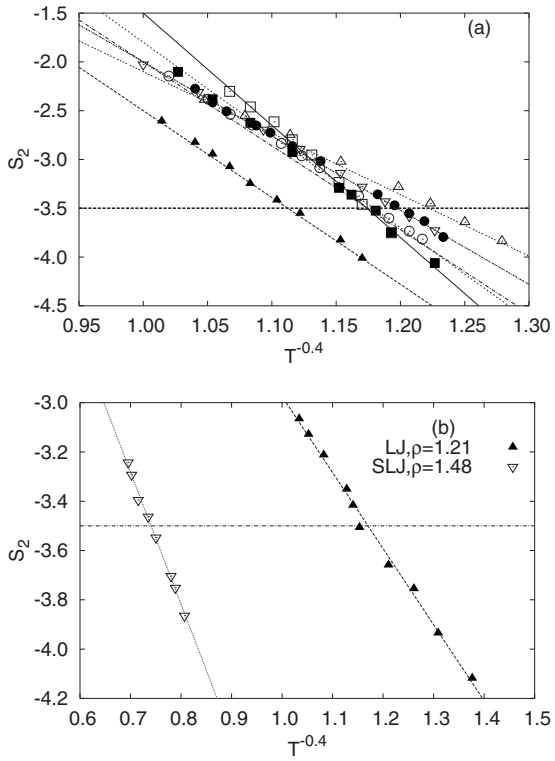

FIG. 4. $T^{-0.4}$ dependence of the pair correlation entropy S_2: (a) M_α, LJ, and SLJ liquids along the $P=0.947$ isobar and (b) LJ and SLJ liquids along $\rho=1.21$ and 1.48 isochores, respectively. Linear fitting parameters are given in Table III. Graphical key for (a) is M_9 (□), M_7 (■), M_6 (○), M_5 (●), M_4 (△), LJ (▲), SLJ (▽).

TABLE III. Parameters for the fitting of the pair correlation entropy S_2 to the functional form $mT^{-0.4}+c$ (see Fig. 4). Numbers in parentheses show the error associated with the last digit.

	System								
Parameter	M_4	M_5	M_6	M_7	M_9	LJ (*NPT*)	SLJ (*NPT*)	LJ (*NVE*)	SLJ (*NVE*)
m	−6.3(1)	−7.6(1)	−8.6(2)	−9.5(2)	−11.5(4)	−8.9(1)	−7.6(1)	−3.09(5)	−5.36(3)
c	4.2(3)	5.6(1)	6.6(2)	7.7(2)	10.0(5)	6.4(2)	5.6(2)	0.11(2)	0.48(3)

fitting parameters have an accuracy of better than 5% for all the systems. In Fig. 4(b), we show that the isochoric data for the LJ and SLJ system also show the $T^{-(2/5)}$ temperature dependence. The isochore for LJ liquid corresponds to the liquid density at the triple point. The isochore for the SLJ liquid corresponds to that studied in Ref. [55]. Thus, the pair correlation entropy S_2 shows the $T^{-0.4}$ dependence of S_2 along both the isochores and isobars, indicating that neglecting the residual entropy term does not have any significant effect on the quantitative temperature dependence. We also show the $T^{3/5}$ dependence of the configurational energy per molecule, $\langle U\rangle/N$, predicted on the basis of density functional theory for Morse and Lennard-Jones liquids, in Fig. 5. We are currently in the process of comparing the temperature dependence of the excess entropy and internal energy for core-softened fluids and ionic melts with waterlike anomalies [61,62].

We show the negative correlation between the translational order τ and S_2 in Fig. 6 which is expected on the basis of the definitions given in Eqs. (2) and (5). Figure 6(a) shows that the $S_2(\tau)$ plots for the Morse and Lennard-Jones systems are nearly superimposable, as seen in the case of $S_2(\rho)$ and $S_2(T)$ curves. Figure 6(b) shows the τ versus S_2 curves for several isotherms of the Lennard-Jones systems. The specific state points correspond to constant densities, rather than pressures. For the $T=0.75$ isotherm, the three points with $S_2 \geqslant -3.0$ correspond to densities in the liquid-vapor coexistence region [63].

Figure 7 shows our results for the correlation of S_2 with the local q_6 bond orientational order parameter. In Fig. 7(a), q_6 is computed using the definition of nearest neighbors as those atoms lying within a cutoff distance R_c corresponding to the location of the first minimum of $g(r)$. With this definition of q_6, S_2 is essentially uncorrelated with the local bond orientational order. For a given value of S_2, the short-range M_9 system has the maximal degree of local order and the long-range M_4 and M_5 liquids have the least. Thus, the bond

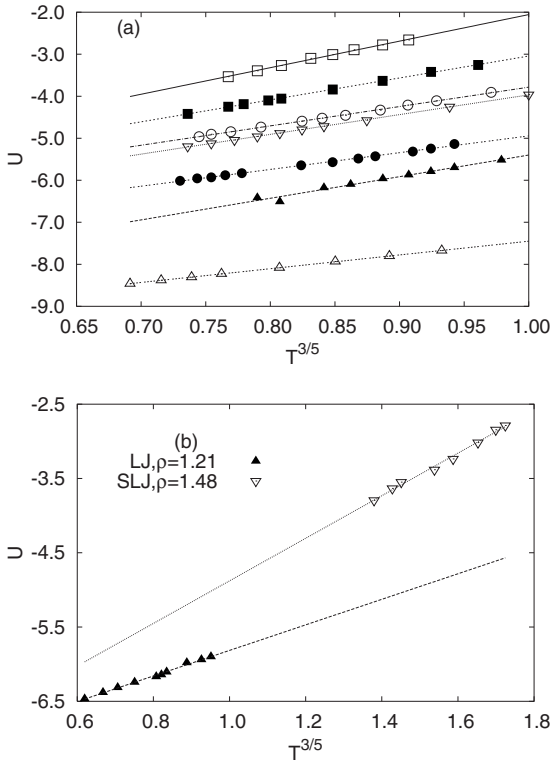

FIG. 5. $T^{3/5}$ dependence of potential energy $\langle U\rangle$ for (a) LJ, M_α, and SLJ liquids along $P=0.947$ isobar and (b) LJ and SLJ liquids along $\rho=1.21$ and 1.48 isochores, respectively. Graphical key for (a) is M_9 (□), M_7 (■), M_6 (○), M_5 (●), M_4 (△), LJ (▲), SLJ (▽).

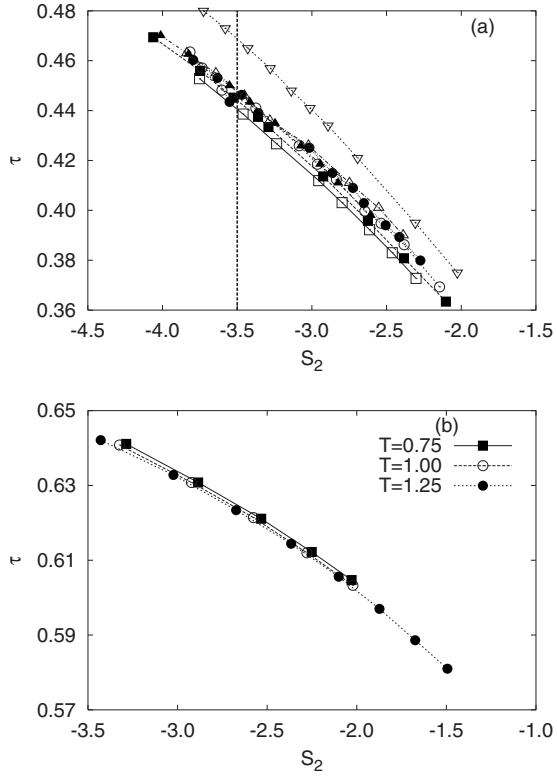

FIG. 6. Dependence of translational order parameter τ on the pair correlation entropy, S_2,: (a) LJ, M_α, and SLJ liquids along $P=0.947$ isobar and (b) LJ and SLJ liquids along $\rho=1.21$ and 1.48 isochores, respectively. Graphical key for (a) is M_9 (□), M_7 (■), M_6 (○), M_5 (●), M_4 (△), LJ (▲), SLJ (▽).

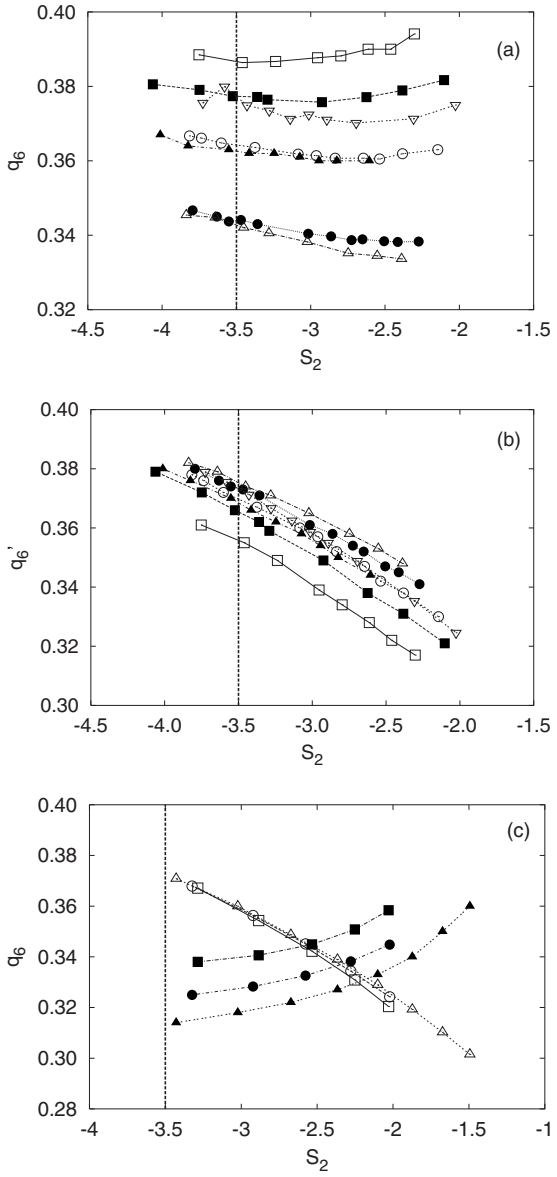

FIG. 7. Dependence of local bond orientational order parameter q_6 or q_6' on pair correlation entropy S_2: (a) q_6 computed using only particles lying closer than first minimum of $g(r)$ for LJ, M_α and SLJ liquids along $P=0.947$ isobar, (b) q_6' computed for 12 closest neighbors for LJ, M_α, and SLJ liquids along $P=0.947$ isobar, Graphical key in (a) and (b) is M_9 (□), M_7 (■), M_6 (○), M_5 (●), M_4 (△), LJ (▲), SLJ (▽). (c) Comparison of q_6' (open symbols) and q_6 (filled symbols) behavior for LJ liquid along three isotherms at $T=0.75$ (□), 1.0 (○), and 1.25 (△).

orientational order associated with the particle arrangements within the nearest-neighbor shell depends on the curvature of the pair interaction but does not alter very significantly with temperature at a given pressure.

In Fig. 7(b), q_6' is computed by summing over the 12 nearest atoms surrounding a given atom, which may include some atoms from the second-neighbor shell, as defined by the peak structure of $g(r)$. In this case, q_6' and S_2 are negatively correlated, with S_2 increasing as q_6 decreases.

The fact that two different definitions of the local order parameter, q_6 and q_6', lead to qualitatively different dependence on the excess entropy is interesting. To examine this issue further, bond orientational order was also calculated for the Lennard-Jones system system simulated under *NVT* conditions along three isotherms for different densities. The resulting q_6 (or q_6') versus S_2 plots are shown in Fig. 7(c). The choice of defining the nearest neighbors as those particles lying within the first minimum of $g(r)$ leads to q_6 versus S_2 curves that are essentially identical for all three isotherms. Moreover, q_6' is negatively correlated with S_2, implying that entropy increases as local order decreases. The q_6 versus S_2 curves, however, show a small positive correlation with entropy. Effectively, the q_6 parameter measures orientational correlations between atoms in the first-neighbor shell whereas q_6' measures orientational correlations between atoms in the first-neighbor shells plus some additional atoms from the next-neighbor shell. q_6' will be affected by the disorder in the first and second shells, and, in addition, will be affected by the partitioning of the 12 molecules between the two subshells. At low S_2 values, $g(r)$ is more structured and the first shell will be more crowded. It is interesting to note that this simple variation in the q_6 definition leads to a qualitatively different dependence on S_2, given the use of these order parameters in the context of core-softened fluids with waterlike anomalies [44,46].

The concept of an ordering map, in which different states of a system are mapped onto a plane whose coordinates are the translation and bond orientational metrics, has proved to be very useful for understanding simple and anomalous liquids. For simple liquids, such as Lennard-Jones and hard-sphere fluids, the two structural metrics are found to be strongly correlated. The crystalline and fluid states map onto distinct regions of the order map. Figures 8(a) and 8(b) plot the order map for the solid state with the x axis of the two plots showing q_6 and q_6', respectively. Since, in the solid phase, the nearest-neighbor shell for fcc solids automatically includes 12 neighbors, the two plots are essentially identical with all the data from the crystalline states of all the systems collapsing onto the same curve on the order map.

Figures 8(c) and 8(d) show the order map for the liquid states, using, respectively, the q_6 and q_6' definitions of bond orientational order. In the liquid state, the τ versus q_6 curves are essentially parallel for different systems with different range and curvature of the potential, as expected on the basis of results shown in Fig. 7. We also note that, in the original work on computing the order map for the Lennard-Jones and hard-sphere systems, the global Q_6, rather than local q_6, bond orientational order was computed, and as a consequence all the τ versus Q_6 plots corresponded to almost vertical lines, with a Q_6 value very close to zero [38].

IV. CONCLUSIONS

The results for Morse and Lennard-Jones liquids presented here demonstrate that the behavior of the pair correlation entropy S_2 at freezing, as well as its temperature dependence, closely follow the predictions made for the excess entropy of pair-additive liquids with purely repulsive interactions. The S_2 value at freezing is $-(3.5\pm0.3)k_B$ for Lennard-Jones, soft-sphere, and Morse liquids. Moreover,

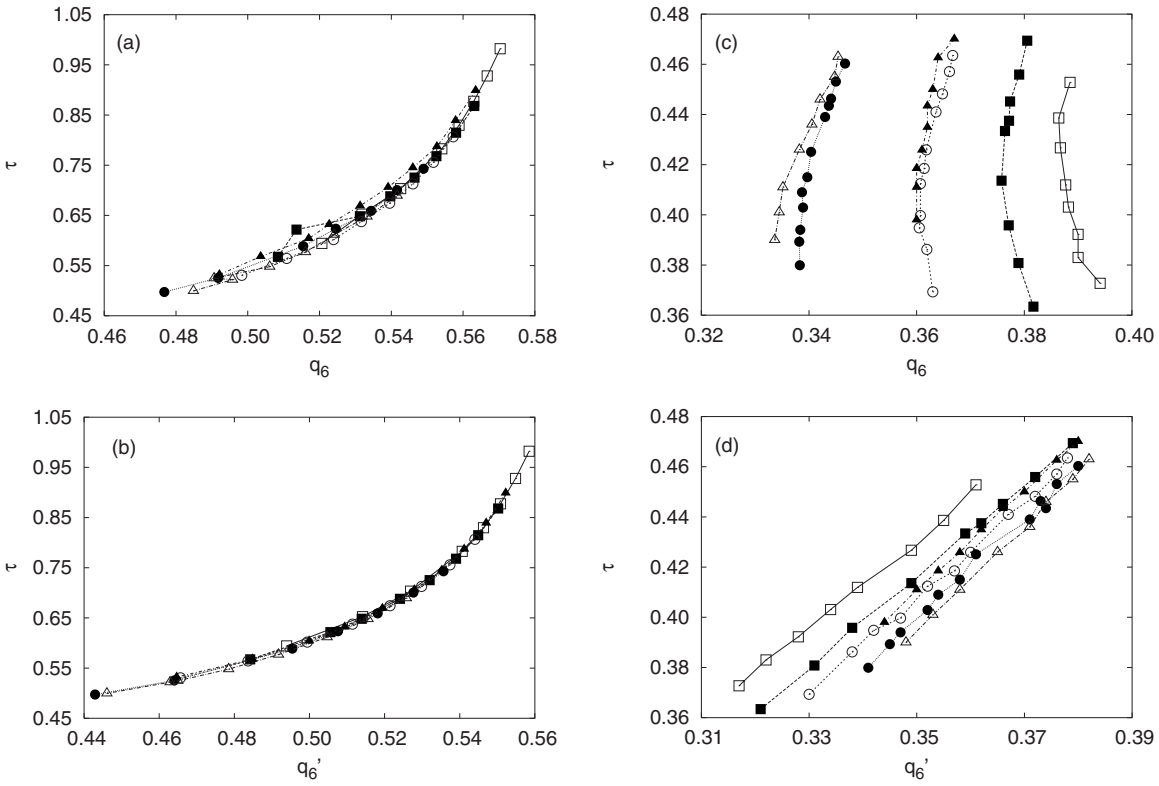

FIG. 8. Correlation between local orientation order q_6 or q_6' and translational order τ for Morse and Lennard-Jones liquids. (a) and (b) correspond to the order maps for the fcc solid. (c) and (d) are order maps for the liquid. Definitions of q_6 and q_6' are as used in Fig. 7. The systems are denoted using the following symbols: M_9 (□), M_7 (■), M_6 (○), M_5 (●), M_4 (△), LJ (▲).

the $T^{-2/5}$ temperature dependence of S_2 is demonstrated for both isobaric as well as isochoric variations in temperature. This provides an additional illustration of the mapping of the behavior of a wide range of simple liquids onto the hard-sphere system, which is interesting in view of the substantial modifications in the potential energy landscape topography of Morse liquids as a function of the nature of range and softness of interactions [13–16]. We are currently examining these relationships for liquids that show waterlike anomalous behavior in comparison to simple liquids [61,62]. In this context, the behavior of complex fluids with ultrasoft repulsions is of particular interest [64–66].

The relationship between the pair correlation entropy (S_2) and local structural order metrics for Morse systems under *NPT* as well as *NVT* conditions is considered in some detail here. S_2 is shown to have a monotonic and negative correlation with the short-range translational order parameter, which is not surprising, since both quantities reflect the degree of structuring of the pair correlation function. The correlation between S_2 and the local bond orientational order is shown to depend on the definition of nearest neighbors used when computing the latter quantity. If the nearest neighbors are those lying within a cutoff distance corresponding to the first minimum in the pair correlation function, then $g(r)$ is weakly correlated with S_2. If the 12 nearest neighbors are considered, then there is a more significant negative correlation. These relationships for the excess entropy are important from the point of view of understanding the origin of various liquid state behaviors that show departures from predictions based on simple liquids. For example, in the case of liquids with waterlike anomalies, it has been demonstrated that the excess entropy is the critical quantity connecting the diffusional, density, and structural anomalies [31]. Moreover, in the case of core-softened fluids with waterlike anomalies, a structurally anomalous regime can be defined only if the local bond orientational order is defined considering the 12 nearest neighbors, presumably because this definition of the order parameter introduces the necessary degree of sensitivity to distortions of icosahedral order. The order map for the Morse liquids is shown to follow the characteristic pattern earlier determined for the hard-sphere and Lennard-Jones systems.

ACKNOWLEDGMENTS

This work was supported by the Department of Science and Technology, New Delhi. SNC thanks the Council for Scientific and Industrial Research, New Delhi, for support.

[1] J. D. Bernal, Proc. R. Soc. London, Ser. A **280**, 138 (1964).
[2] J.-P. Hansen and I. R. McDonald, *Theory of Simple Liquids* (Academic Press, New York, 1986).
[3] H. Lowen, Phys. Rep. **237**, 249 (1994).
[4] P. A. Monson and D. A. Kofke, Adv. Chem. Phys. **115**, 113 (2000).
[5] V. G. Fastovskii, A. E. Rovinskii, and Y. V. Petrovskii, *Inert Gases* (Israel Program for Scientific Translation, Jerusalem, 1967).
[6] M. Shimoji, *Liquid Metals: An Introduction to the Physics and Chemistry of Metals in the Liquid State* (Academic Press, London, 1977).
[7] S. N. Chakraborty, N. Ghosh, P. Shah, and C. Chakravarty, Mol. Phys. **102**, 909 (2004).
[8] P. M. Morse, Phys. Rev. **34**, 57 (1929).
[9] D. J. Wales, *Energy Landscapes: With Applications to Clusters, Biomolecules and Glasses* (Cambridge University Press, Cambridge, U.K., 2003).
[10] L. A. Girifalco and V. G. Weizer, Phys. Rev. **114**, 687 (1959).
[11] D. J. Wales, L. J. Munro, and J. P. K. Doye, J. Chem. Soc. Dalton Trans. **1996**, 611.
[12] J. P. K. Doye and D. J. Wales, Science **271**, 484 (1996).
[13] P. Shah, P. Chakraborty, and C. Chakravarty, Mol. Phys. **99**, 573 (2001).
[14] P. Shah and C. Chakravarty, Phys. Rev. Lett. **88**, 255501 (2002).
[15] P. Shah and C. Chakravarty, J. Chem. Phys. **116**, 10825 (2002).
[16] P. Shah, S. Roy, and C. Chakravarty, J. Chem. Phys. **118**, 10671 (2003).
[17] R. E. Nettleton and M. S. Green, J. Chem. Phys. **29**, 1365 (1958).
[18] D. C. Wallace, J. Chem. Phys. **87**, 2282 (1987).
[19] A. Baranyai and D. J. Evans, Phys. Rev. A **40**, 3817 (1989).
[20] A. Baranyai and D. J. Evans, Phys. Rev. A **42**, 849 (1990).
[21] T. Lazaridis and M. E. Paulaitis, J. Phys. Chem. **96**, 3847 (1992).
[22] B. B. Laird and A. D. J. Haymet, Phys. Rev. A **45**, 5680 (1992).
[23] Y. Rosenfeld, Mol. Phys. **32**, 963 (1976).
[24] Y. Rosenfeld, Phys. Rev. A **15**, 2545 (1977); Chem. Phys. Lett. **48**, 467 (1977).
[25] Y. Rosenfeld, Phys. Rev. A **26**, 3633 (1982).
[26] Y. Rosenfeld, J. Phys.: Condens. Matter **11**, 5415 (1999).
[27] Y. Rosenfeld, Phys. Rev. E **62**, 7524 (2000).
[28] M. Dzugutov, Nature (London) **381**, 137 (1996).
[29] J. Mittal, J. R. Errington, and T. M. Truskett, J. Chem. Phys. **125**, 076102 (2006).
[30] J. Mittal, J. R. Errington, and T. M. Truskett, J. Phys. Chem. B **110**, 18147 (2006).
[31] R. Sharma, S. N. Chakraborty, and C. Chakravarty, J. Chem. Phys. **125**, 204501 (2006).
[32] J. Mittal, J. R. Errington, and T. M. Truskett, J. Chem. Phys. **125**, 244502 (2006).
[33] S. N. Chakraborty and C. Chakravarty, J. Chem. Phys. **124**, 014507 (2006).
[34] S. Torquato, T. M. Truskett, and P. G. Debenedetti, Phys. Rev. Lett. **84**, 2064 (2000).
[35] T. M. Truskett, S. Torquato, and P. G. Debenedetti, Phys. Rev. E **62**, 993 (2000).
[36] A. R. Kansal, S. Torquato, and F. H. Stillinger, Phys. Rev. E **66**, 041109 (2002).
[37] S. Torquato, Annu. Rev. Mater. Res. **32**, 77 (2002).
[38] J. E. Errington, P. G. Debenedetti, and S. Torquato, J. Chem. Phys. **118**, 2256 (2003).
[39] P. J. Steinhardt, D. R. Nelson, and M. Ronchetti, Phys. Rev. B **28**, 784 (1983).
[40] U. Gasser, A. Schofield, and D. A. Weitz, J. Phys.: Condens. Matter **15**, S375 (2003).
[41] J. R. Errington and P. G. Debenedetti, Nature (London) **409**, 318 (2001).
[42] M. S. Shell, P. G. Debenedetti, and A. Z. Panagiotopoulos, Phys. Rev. E **66**, 011202 (2002).
[43] Z. Yan, S. V. Buldyrev, N. Giovambattista, and H. E. Stanley, Phys. Rev. Lett. **95**, 130604 (2005).
[44] P. Kumar, S. V. Buldyrev, F. Sciortino, E. Zaccarelli, and H. E. Stanley, Phys. Rev. E **72**, 021501 (2005).
[45] Z. Yan, S. V. Buldyrev, N. Giovambattista, P. G. Debenedetti, and H. E. Stanley, Phys. Rev. E **73**, 051204 (2006).
[46] A. B. de Oliveira, P. A. Netz, T. Colla, and M. C. Barbosa, J. Chem. Phys. **124**, 084505 (2006).
[47] L. Xu, S. V. Buldyrev, C. A. Angell, and H. E. Stanley, Phys. Rev. E **74**, 031108 (2006).
[48] P. V. Giaquinta, G. Giunta, and S. P. Prestipino Giarritta, Phys. Rev. A **45**, R6966 (1992).
[49] P. V. Giaquinta and G. Giunta, Physica A **187**, 145 (1992).
[50] F. Saija, S. Prestipino, and P. V. Giaquinta, J. Chem. Phys. **115**, 7586 (2001).
[51] F. Saija, S. Prestipino, and P. V. Giaquinta, J. Chem. Phys. **124**, 244504 (2006).
[52] I. Yokoyama, Physica B **254**, 172 (1998).
[53] J.-P. Hansen and L. Verlet, Phys. Rev. **184**, 151 (1969).
[54] R. Agrawal and D. A. Kofke, Mol. Phys. **85**, 43 (1995).
[55] R. A. LaViolette and F. H. Stillinger, J. Chem. Phys. **83**, 4079 (1985).
[56] M. D. Allen and D. J. Tildesley, *Computer Simulation of Liquids* (Clarendon Press, Oxford, 1986).
[57] D. Frenkel and B. Smit, *Understanding Molecular Simulation: From Algorithms to Applications* (Academic Press, London, 2002).
[58] C. Chakravarty, P. G. Debenedetti, and F. H. Stillinger (unpublished).
[59] R. Agrawal and D. A. Kofke, Mol. Phys. **85**, 23 (1995).
[60] S. N. Chakraborty and C. Chakravarty, J. Chem. Phys. **126**, 244512 (2007).
[61] M. Agarwal, R. Sharma, and C. Chakravarty (unpulished).
[62] R. Sharma and C. Chakravarty, J. Chem. Phys. (to be published).
[63] B. Smit, J. Chem. Phys. **96**, 8639 (1992).
[64] M. Watzlawek, C. N. Likos, and H. Lowen, Phys. Rev. Lett. **82**, 5289 (1999).
[65] C. N. Likos, N. Hoffann, H. Lowen, and A. A. Louis, J. Phys.: Condens. Matter **14**, 7681 (2002).
[66] M. C. Rechtsman, F. H. Stillinger, and S. Torquato, Phys. Rev. E **75**, 031403 (2007).